Axial dispersion via shear-enhanced diffusion in colloidal suspensions

Axial dispersion via shear-enhanced diffusion in colloidal suspensions

I. M. Griffiths[1,2(a)] and H. A. Stone[1]

[1] *Department of Mechanical and Aerospace Engineering, Princeton University - Princeton, NJ 08544, USA*
[2] *OCCAM, Mathematical Institute, University of Oxford - Oxford, OX1 3LB, UK, EU*

Abstract – The familiar example of Taylor dispersion of molecular solutes is extended to describe colloidal suspensions, where the fluctuations that contribute to dispersion arise from hydrodynamic interactions. The generic scheme is illustrated for a suspension of particles in a pressure-driven pipe flow, with a concentration-dependent diffusivity that captures both the shear-induced and Brownian contributions. The effect of the cross-stream migration via shear-induced diffusion is shown to dramatically reduce the axial dispersion predicted by classical Taylor dispersion for a molecular solute. Analytic and numerical solutions are presented that illustrate the effect of the concentration dependence of this nonlinear hydrodynamic mechanism.

Colloidal suspensions are ubiquitous in everyday life, as they occur in many applications of soft materials [1], drug delivery systems [2], environmental science (*e.g.*, filtration and water purification), and the flow of physiological fluids such as blood. The subject has been given renewed emphasis owing to the control offered by microfluidic devices for manipulating the flow of complex liquids [3]. In many cases, one suspension is injected into another, either in a continuous fashion or as a localized bolus.

The transport features of a suspension, such as the spreading of the injected pulse along the flow direction, are of significant interest. Traditionally, such dispersion problems are analysed assuming thermal fluctuations are the driving force for sampling the velocity distribution. For sufficiently strong shear rates in the flow, hydrodynamic effects will always dominate thermal effects, and so here we analyse the influence of hydrodynamic interactions on such dispersion problems.

It is well known that in a thin channel axial spreading of a molecular solute occurs as a consequence of a non-uniform velocity distribution in the direction transverse to the mean flow [4,5]. Taylor dispersion refers to the common case where thermal diffusion is the source of the fluctuations that lead to sampling of the streamlines and dictates the magnitude of axial dispersion. The usual approach to

axial-dispersion problems is to seek a description in terms of a one-dimensional convective-diffusion equation, with the goal being to determine the effective diffusivity. In particular, for a circular channel of radius R, or a rectangular channel of height R much less than the width, the mechanical contribution to the spreading has the order of magnitude $O(\bar{u}^2 R^2 / D_m)$, where $\bar{u}$ represents the average flow velocity and D_m is the molecular-diffusion coefficient. For typical flow conditions, this mechanical spreading dominates the molecular diffusion and is the principal contributor to the axial spread of the solute. To accurately model the distribution of finite-sized particulates in a similar geometry requires a theory that captures the influence of hydrodynamic interactions on dispersion. In this case, determining the functional dependence of the axial-dispersion coefficient on particle concentration is key.

For common flow conditions of a colloidal suspension, shear-induced diffusion, which is a consequence of hydrodynamic interactions between particles and is dependent on their concentration, dominates over thermal fluctuations (Brownian motion). While there are many variants of the Taylor-dispersion problem (*e.g.*, [6]), almost all consider only problems that assume the stochastic element driving solutes across streamlines, transverse to the flow direction, is Brownian motion. The shear-induced diffusion of colloids across streamlines gives rise to a *shear-enhanced diffusion* in the axial flow direction analogous to

---
[(a)]E-mail: ian.griffiths@maths.ox.ac.uk

Taylor dispersion that describes the observed enhanced axial diffusion of a molecular solute. In this letter we examine the effect of the shear-induced diffusion upon the observed dispersion. This description leads to a nonlinear convection-diffusion equation, with an explicit expression for the diffusivity dependence on particle concentration. We solve a simplified model analytically for low particle concentrations and numerically for higher concentrations.

Two relevant particle diffusivities may be identified when dealing with colloidal suspensions: the self-diffusivity of an individual tracer particle within a homogeneous suspension, and the collective, or down-gradient, diffusivity [7]. The collective diffusivity arises as a response to a concentration gradient in a shear flow, with the higher concentration of particles producing more "collisions" so that there is a systematic cross-streamline migration of particles to regions of lower concentrations.

The shear-induced self-diffusion of particles has been studied experimentally [8], theoretically [9–11] and computationally [12]. In a unidirectional flow, the characteristic shear-induced self-diffusivity for spherical particles is proportional to the local shear rate, $\dot{\gamma}$, the square of the particle radius, a, and a proportionality factor that is a function of the volume fraction of particles, which itself is related to the colloidal mass concentration, c [8,13]. While self-diffusion coefficients can be calculated using appropriate kinematic descriptions, computation of the collective diffusivity is more complex. The collective diffusivity has been studied theoretically and computationally (see, for example, [7,9,14,15]), which suggests an approximate linear relationship between the collective and self-diffusivities, and thus an equivalent dependence on the system parameters.

Due to the linearity and time reversibility of the Stokes flow, a purely hydrodynamic collision between two smooth non-colloidal spheres is symmetrical: the particles return to their original streamlines after the passing encounter. Thus, at least three spheres must interact to have a net displacement and, consequently, the shear-induced component of diffusivity is expected to scale as c^2 for low concentrations [14,16]. Non-hydrodynamic interactions such as repulsive forces, particle roughness or symmetry breaking, as in the case of non-spherical particles, lead to a diffusivity that is linear in c in the dilute limit [9,17,18].

The coupling between Brownian and hydrodynamic forces due to shearing motion is non-trivial. The theory we present here is valid for any functional form for the diffusivity, but we assume that the effects are additive and the collective diffusivity is represented as

$$D(c) = D_m + a^2|\dot{\gamma}|f(c), \qquad (1)$$

where $f(c)$ is a dimensionless function of colloidal concentration. For spherical particles, D_m is given by the Stokes-Einstein relation, $D_m = k_B T/6\pi\mu a$, where k_B is the Boltzmann constant, T is the temperature and μ is the viscosity of the fluid in which the colloids are suspended. We emphasize that the steps in our
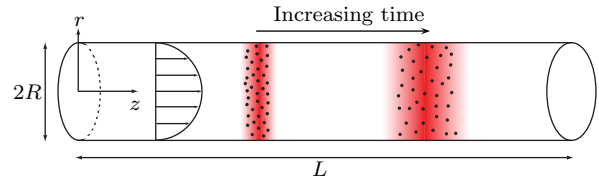

Fig. 1: (Colour on-line) Schematic diagram for the axial spreading of a pulse of particles in the pressure-driven pipe flow of a colloidal suspension.

analysis hold for more complex expressions for the diffusivity that capture the coupling between molecular and shear-induced diffusion, but eq. (1) displays the correct asymptotic behaviour in the limit of large and small colloidal sizes and shear rates. Under common flow conditions in colloidal suspensions the shear-induced diffusion will dominate over the molecular diffusion. For weakly sheared suspensions the collective diffusivity may also depend linearly on the particle-scale Péclet number based on the average shear rate, $|\dot{\gamma}|a^2/D_m$ [19]. Such additional parametric dependence can be incorporated into the functional form of f.

We consider the effect of a shear-induced diffusivity on the dispersion of a colloidal suspension when placed in a steady pressure-driven pipe flow. We suppose that the pipe has radius R and length L and use an axisymmetric cylindrical coordinate system (r, z) to describe the flow, with z directed along the length of the pipe, as depicted in fig. 1.

For low colloidal concentrations, the laminar pressure-driven axial velocity profile is given by

$$u(r) = 2\overline{u}(1 - (r/R)^2), \qquad (2)$$

where $\overline{u}$ is the radially averaged velocity, defined by

$$\overline{u} = \frac{2}{R^2} \int_0^R u(r)\, r\mathrm{d}r, \qquad (3)$$

and the corresponding shear rate $\dot{\gamma} = \partial u/\partial r = -4\overline{u}r/R^2$. Adjustments to the viscosity that arise as a result of the small differences in concentration will induce higher-order corrections to the velocity profile from the Poiseuille form (2) which we neglect here. The axisymmetric colloidal mass concentration, $c(r, z, t)$, is then governed by the advection-diffusion equation,

$$\frac{\partial c}{\partial t} + u\frac{\partial c}{\partial z} = \frac{1}{r}\frac{\partial}{\partial r}\left(rD\frac{\partial c}{\partial r}\right) + \frac{\partial}{\partial z}\left(D\frac{\partial c}{\partial z}\right), \qquad (4)$$

where $D(c)$ is given by (1). Following the approach of Taylor [4], we work in terms of deviations from cross-sectionally averaged quantities, defined in (3), writing $c = \overline{c}(z, t) + c'(r, z, t)$ and $u = \overline{u} + u'(r)$. Substituting into (4) gives

$$\frac{\partial \overline{c}}{\partial t} + \frac{\partial c'}{\partial t} + \overline{u}\frac{\partial \overline{c}}{\partial z} + u'\frac{\partial \overline{c}}{\partial z} + \overline{u}\frac{\partial c'}{\partial z} + u'\frac{\partial c'}{\partial z} =$$
$$\frac{1}{r}\frac{\partial}{\partial r}\left(rD\frac{\partial c'}{\partial r}\right) + \frac{\partial}{\partial z}\left(D\frac{\partial \overline{c}}{\partial z}\right) + \frac{\partial}{\partial z}\left(D\frac{\partial c'}{\partial z}\right). \qquad (5)$$

Equation (5) is averaged over the tube cross-section to provide

$$\frac{\partial \overline{c}}{\partial t} + \overline{u}\frac{\partial \overline{c}}{\partial z} + \overline{u'\frac{\partial c'}{\partial z}} = \frac{\partial}{\partial z}\left(\overline{D}\frac{\partial \overline{c}}{\partial z}\right) + \frac{\partial}{\partial z}\left(\overline{D\frac{\partial c'}{\partial z}}\right), \quad (6)$$

which may be subtracted from (5) to give

$$\frac{\partial c'}{\partial t} + u'\frac{\partial \overline{c}}{\partial z} + \overline{u}\frac{\partial c'}{\partial z} + u'\frac{\partial c'}{\partial z} - \overline{u'\frac{\partial c'}{\partial z}} = \frac{1}{r}\frac{\partial}{\partial r}\left(rD\frac{\partial c'}{\partial r}\right)$$

$$+ \frac{\partial}{\partial z}\left((D - \overline{D})\frac{\partial \overline{c}}{\partial z}\right) + \frac{\partial}{\partial z}\left(D\frac{\partial c'}{\partial z}\right) - \frac{\partial}{\partial z}\left(\overline{D\frac{\partial c'}{\partial z}}\right). \tag{7}$$

We are interested in the long-time behaviour of cross-stream diffusion, that is, $L \gg \overline{u}R^2/D$, and we suppose that $|c'|/\overline{c} \ll 1$ so that deviations in concentration from the mean are small, under which assumptions (6) and (7) simplify to

$$\frac{\partial \overline{c}}{\partial t} + \overline{u}\frac{\partial \overline{c}}{\partial z} \approx \frac{\partial}{\partial z}\left(\overline{D}(\overline{c})\frac{\partial \overline{c}}{\partial z}\right) - \overline{u'\frac{\partial c'}{\partial z}}, \tag{8}$$

and

$$\frac{1}{r}\frac{\partial}{\partial r}\left(rD(\overline{c})\frac{\partial c'}{\partial r}\right) \approx u'\frac{\partial \overline{c}}{\partial z}, \tag{9}$$

respectively. Equation (8) corresponds to the generalization for a spatially dependent diffusivity of the usual Taylor-dispersion result. As usual, the mechanical contribution to the effective diffusion of the colloids arises in (8) from the "fluctuation"-generated flux $\overline{u'\partial c'/\partial z}$. The influence of the shear-enhanced diffusivity enters through the functional form of this term. Use of (9) and integration by parts gives

$$\overline{u'\frac{\partial c'}{\partial z}} = -\frac{\overline{u}^2 R^2}{D_m}\frac{\partial}{\partial z}\left(\mathcal{D}(\overline{c})\frac{\partial \overline{c}}{\partial z}\right), \tag{10}$$

where the dimensionless dispersion coefficient $\mathcal{D}(\overline{c})$ is given by

$$\mathcal{D}(\overline{c}) = \frac{2D_m}{\overline{u}^2 R^2}\int_0^R \left(\int_0^r \hat{r}u'(\hat{r})\,\mathrm{d}\hat{r}\right)^2 \frac{\mathrm{d}r}{rD(\overline{c})}. \tag{11}$$

Equation (11) may be evaluated explicitly for the specific velocity $u' = \overline{u}(1 - 2(r/R)^2)$ and functional form for the diffusivity (1) to give

$$\mathcal{D}(\overline{c}) \equiv \frac{1}{2F^7} - \frac{1}{4F^6} - \frac{5}{6F^5} + \frac{3}{8F^4} + \frac{4}{15F^3} - \frac{1}{12F^2}$$

$$+ \frac{4}{105F} - \frac{\ln(1+F)}{2F^8} + \frac{\ln(1+F)}{F^6} - \frac{\ln(1+F)}{2F^4}, \tag{12}$$

where $F(\overline{c}) = 3Pe_s f(\overline{c})/2$, f is defined in (1) and

$$Pe_s = \frac{|\overline{\dot{\gamma}}|a^2}{D_m} = \frac{8\overline{u}a^2}{3RD_m} \tag{13}$$

is the particle-scale Péclet number based on the average shear rate.

In the limit when $F \ll 1$, the shear-enhanced component of diffusion is negligible and we recover the usual Taylor-dispersion result for the dispersion coefficient, $\mathcal{D} \sim 1/48$. However, when $F \gg 1$ and the diffusion is dominated by the shear-induced contribution, we obtain the leading-order result

$$\mathcal{D}(\overline{c}) \sim \frac{4}{105F(\overline{c})} = \frac{4}{105Pe_s f(\overline{c})}. \tag{14}$$

Since $F(\overline{c}) \gg 1$, the modified dispersivity $\mathcal{D} \ll 1$, and thus we find, crucially, that the enhanced cross-stream migration as a result of shear-induced diffusion severely reduces the axial dispersion. The coefficient $4/105$ is equivalent to that obtained for Taylor dispersion in a unidirectional parabolic channel flow between two parallel plates, though this appears only coincidental. The effective diffusivity $\overline{u}^2 R^2 \mathcal{D}/D_m \sim \overline{u}R^3/70a^2 f(\overline{c})$, and thus depends linearly upon axial velocity as is the case for dispersion in a porous rock for large pore Péclet numbers.

Converting to a dimensionless coordinate frame that convects with the mean fluid velocity, $Ls = z - \overline{u}t$, and letting $t = D_m L^2 \tau/\overline{u}^2 R^2$ and $\overline{c} = MC/\pi R^2 L$, where

$$M = \pi R^2 \int_{-\infty}^{\infty} \overline{c}\,\mathrm{d}z \tag{15}$$

is the total number of colloids in the flow, from (8) we arrive at the non-dimensional equation for the colloidal concentration,

$$\frac{\partial C}{\partial \tau} = \frac{\partial}{\partial s}\left(\left(\frac{1}{Pe^2}\left(1 + Pe_s f(C)\right) + \mathcal{D}(C)\right)\frac{\partial C}{\partial s}\right), \tag{16}$$

where $Pe = \overline{u}R/D_m$ is the Péclet number based on the tube radius.

During one shear time ($1/|\overline{\dot{\gamma}}| = 3R/8\overline{u}$) a single particle will pass another and be displaced randomly by one particle radius across the streamlines, while travelling a mean axial distance $3R/8$. A total of R/a steps in one direction are required for the particle to travel across the entire tube cross-section, and since these steps occur randomly in both directions, a total of $(R/a)^2$ steps are required to sample the entire cross-section. This estimate leads to the *correlation distance*,

$$L_c = \frac{3R}{8}\frac{R^2}{a^2} = \frac{3R^3}{8a^2}, \tag{17}$$

which provides the axial distance travelled during which particles sample the entire tube cross-section. Thus, for $10\,\mu\text{m}$ particles in a tube with cross-sectional radius $200\,\mu\text{m}$ the effects of shear-enhanced diffusion will be observed over an axial distance of the order of $3\,\text{cm}$.

In table 1 we list typical parameters for an appropriate microfluidic device configuration. For all particle sizes of interest, $Pe \gg 1$, so we henceforth focus on the limit

Table 1: Typical operating parameters for $CaCO_3$ particles in water and at room temperature ($\mu = 8.9 \times 10^{-4}\,\mathrm{Pa\,s}$ and $T = 298\,\mathrm{K}$) [18,20].

a	R	L
$10\,\mu\mathrm{m}$	$200\,\mu\mathrm{m}$	$3\,\mathrm{cm}$
$\overline{u}$	Pe_s	Pe
$1\,\mathrm{mm\,s^{-1}}$	$\approx 5 \times 10^4$	$\approx 8 \times 10^6$

in which the dominant contribution to the diffusivity in (16) arises from the fluctuation-generated term, $\mathcal{D}$. We note that the molecular and shear-induced radial diffusivities are respectively, $O(1/Pe^2)$ and $O(Pe_s/Pe^2)$ weaker than the axial diffusion so our assumption that the concentration variations in the radial direction are small is justified.

For dilute systems, the shear-induced diffusivity for perfectly smooth spherical colloids scales as C^2, while symmetry breaking or surface roughness leads to diffusivities that are linear in C [9,17]. We therefore begin by examining the resulting shear-induced dispersion in the dilute limit when $f(\overline{c}) = AC^n$ for an arbitrary n, where A is a constant. Provided C does not become too small (order $1/Pe_s$), so that F remains large, we may use the simplified expression (14) for the diffusivity. The colloidal concentration is then governed by

$$\frac{\partial C}{\partial \tau} = \frac{\partial}{\partial s}\left(\frac{1}{C^n}\frac{\partial C}{\partial s}\right) \tag{18}$$

(where we have absorbed the constant $1/(105APe_s)$ into the time variable τ), which we recognize as a version of the porous medium equation.

For an instantaneous pulse of particles injected into the flow at $s = 0$ and $\tau = 0$, the solution to (18) that conserves the total number of particles takes the form

$$C(s,\tau) = \frac{\psi(\xi_n)}{\tau^{1/(2-n)}}, \tag{19}$$

where $\xi_n = s/\tau^{1/(2-n)}$, for $0 < n < 2$. This solution form may be substituted into (18) and integrated twice to give

$$\psi(\xi_n) = \left(\frac{n}{2(2-n)}\left(\alpha_n + \xi_n^2\right)\right)^{-1/n}, \tag{20}$$

where we have used the symmetry boundary condition $\psi'(0) = 0$. Here, α_n is a constant that may be determined by conservation of mass,

$$\int_{-\infty}^{\infty} C\,\mathrm{d}s = \int_{-\infty}^{\infty} \psi\,\mathrm{d}\xi_n = 1, \tag{21}$$

which gives

$$\alpha_n = \left(\frac{4-2n}{n}\right)^{\frac{2}{2-n}}\left(\frac{\Gamma(1/n)}{\sqrt{\pi}\Gamma(1/n - 1/2)}\right)^{-\frac{2n}{2-n}}. \tag{22}$$

Thus, the concentration is given by

$$C(s,\tau) = \left[\frac{n}{2(2-n)}\left(\alpha_n\tau^{n/(2-n)} + \frac{s^2}{\tau}\right)\right]^{-1/n}, \tag{23}$$
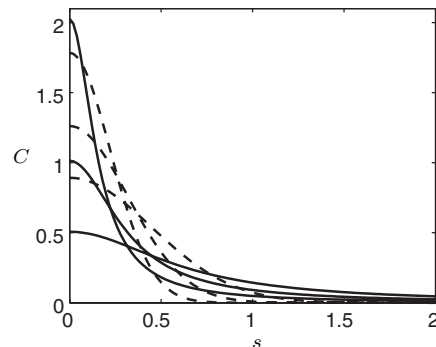
for $0 < n < 2$.

Fig. 2: Comparison between the diffusion of a pulse of particles given by (23) when $n = 1$ (solid lines) with the solution for regular diffusion, $C = \mathrm{e}^{-s^2/4\tau}/(2\sqrt{\pi\tau})$ (dashed lines) at $\tau = 0.025, 0.05, 0.1$.

We can compare (23) with the solution for diffusion of a pulse with constant (unit) diffusivity, which is familiar in Taylor dispersion of molecular solutes,

$$C(s,\tau) = \frac{\mathrm{e}^{-s^2/4\tau}}{2\sqrt{\pi\tau}}. \tag{24}$$

In both cases, the spread advances in space as the square root of time, through the term s^2/τ. However, in (23) the spreading occurs algebraically with the height of the peak decaying as $\tau^{-1/(2-n)}$, while (24) displays an exponential spreading, with the height of the peak decaying as $\tau^{-1/2}$.

The time evolution of the solution to (18) when $n = 1$, given by (23), is compared in fig. 2 with the solution for diffusion of a pulse with unit diffusivity, when $n = 0$, given by (24). As a result of the stronger effective diffusivity in the former, the concentration distribution is smoothed out much more quickly, with the height of the peaks obeying τ^{-1} and $\tau^{-1/2}$ decay laws, respectively.

The solution (23) clearly breaks down for $n = 2$, which corresponds to the shear-enhanced diffusion of perfectly spherical particles at low concentrations lacking non-hydrodynamic interactions. In this case, the similarity solution takes the form [21,22]

$$C(s,\tau) = \mathrm{e}^{-\omega\tau}\psi(\xi_2), \tag{25}$$

where $\xi_2 = s\mathrm{e}^{-\omega\tau}$ and ω is an, as yet, undetermined constant. Substituting (25) into (18) provides $\psi(\xi_2) = (\alpha_2 + \omega\xi_2^2)^{-1/2}$, where α_2 is a constant of integration, and so

$$C(s,\tau) = \exp(-\omega\tau)\left(\alpha_2 + \omega s^2\mathrm{e}^{-2\omega\tau}\right)^{-1/2}. \tag{26}$$

However, the total mass associated with this solution (and (23) for $n > 2$) is unbounded. This feature arises as a result of our simplified expression for $\mathcal{D}$, which is no longer valid when C becomes small and F becomes order one. In such regions, all terms in (12) are important, and ensure that the diffusivity remains bounded as $C \to 0$. We thus conclude that the respective solutions (23) for $n > 2$
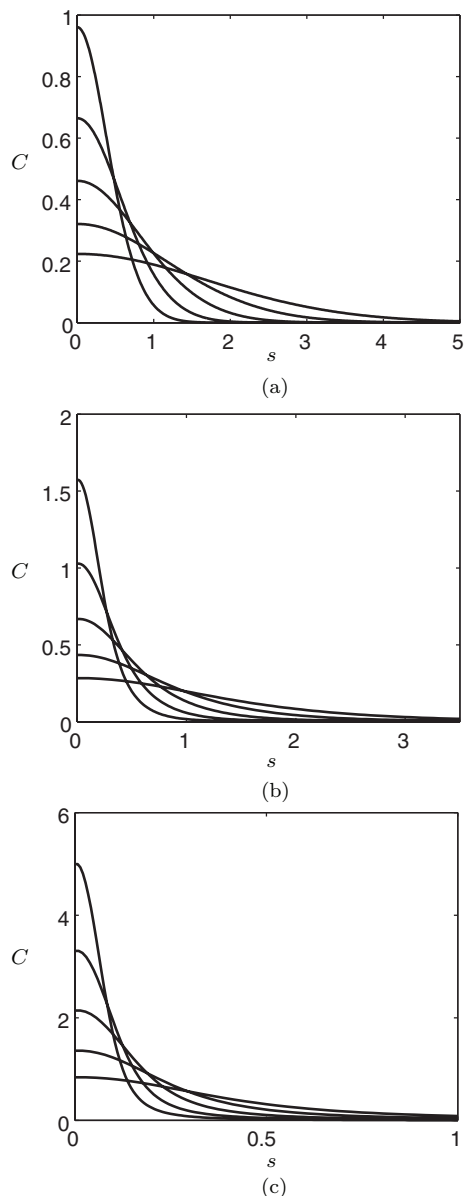
(a)

(b)

(c)

Fig. 3: Concentration distribution, C, *vs.* s given by (16) with (27) at $\tau = 5, 10, 20, 40, 80$ with $A = \beta = 1$ and (a) $Pe_s = 1$, (b) $Pe_s = 10$, (c) $Pe_s = 100$. In all cases the arrows indicate the direction of increasing τ.

and (26) for $n = 2$ provide the behaviour in regions where the concentration is suitably larger than $O(1/Pe_s)$, but the behaviour in the tail regions of the profile, where C becomes small, is determined by using the full expression for the diffusivity, eq. (12). The constants ω and α_2 in (26) are then, in principle, determined by matching together the solutions in these two regions, and enforcing conservation of mass. Nevertheless, we observe that when $n = 2$ particles now diffuse with an exponential rather than an algebraic spread with time in regions where the colloidal concentration is not too small. We note also that, when $n = 2$, eq. (18) may be transformed to the regular diffusion equation via a contact transformation [23].

While the shear-induced component of diffusivity depends typically linearly or quadratically on concentration for low concentrations, as we increase the colloidal concentration, the diffusivity saturates [13]. Thus, we now consider a model with the more general functional form,

$$f = \frac{AC}{1 + \beta C}, \qquad A, \beta = \text{constant}. \qquad (27)$$

The solution of (16) with (27) may be determined numerically. For computational simplicity, we approximate the initial pulse of colloidal particles as a Gaussian distribution of the form $C(s, 0) = \mathrm{e}^{-s^2/\tau_0}/\sqrt{\pi\tau_0}$, where $\tau_0 \ll 1$. In fig. 3 we illustrate the time evolution of a pulse of colloidal particles with $\tau_0 = 10^{-4}$, when $A = \beta = 1$ and $Pe_s = 1, 10, 100$. While these results illustrate the behaviour, this model may be improved by including the dependence of viscosity upon concentration, which will enter through a modification in $f(c)$.

In summary, the results reported here demonstrate that the hydrodynamic interactions that drive fluctuations in the concentration of a colloidal suspension yield a nonlinear transport process. The behaviour depends on the explicit features characterizing the functional relation between shear-induced diffusivity and colloidal concentration. The axial dispersion, or shear-enhanced diffusion, that arises as a result of the additional shear-induced cross-stream migration, is shown to be dramatically reduced when compared with the Taylor-dispersion result for that of a molecular solute. The approach presented may be used to refine the standard dispersion methods used to determine the diffusion coefficients for colloids and nanoparticles (see, for example, [24,25]).

$* * *$

REFERENCES

[1] Russel W. B., Saville D. A. and Schowalter W. R., *Colloidal Dispersions* (Cambridge University Press) 1992.
[2] Shipley R. J., Waters S. L. and Ellis M. J., *Biotech. Bioeng.*, **107** (2011) 382.
[3] Squires T. M. and Quake S. R., *Rev. Mod. Phys.*, **77** (2005) 977.
[4] Taylor G., *Proc. R. Soc. A*, **219** (1953) 186.

[5] Aris R., *Proc. R. Soc. A*, **38** (1956) 67.

[6] Brenner H. and Edwards D. A., *Macrotransport Processes* (Butterworth-Heinemann) 1993.

[7] Leshansky A. M. and Brady J. F., *J. Fluid Mech.*, **527** (2005) 141.

[8] Eckstein E. C., Bailey D. G. and Shapiro A. H., *J. Fluid Mech.*, **79** (1977) 191.

[9] Da Cunha F. R. and Hinch E. J., *J. Fluid Mech.*, **309** (1996) 211.

[10] Wang Y., Mauri R. and Acrivos A., *J. Fluid Mech.*, **327** (1996) 255.

[11] Acrivos A., Batchelor G. K., Hinch E. J., Koch D. L. and Mauri R., *J. Fluid Mech.*, **240** (1992) 651.

[12] Sierou A. and Brady J. F., *J. Fluid Mech.*, **506** (2004) 285.

[13] Leighton D. and Acrivos A., *J. Fluid Mech.*, **181** (1987) 415.

[14] Wang Y., Mauri R. and Acrivos A., *J. Fluid Mech.*, **357** (1998) 279.

[15] Marchioro M. and Acrivos A., *J. Fluid Mech.*, **443** (2001) 101.

[16] Leighton D. and Acrivos A., *J. Fluid Mech.*, **177** (1986) 109.

[17] Lopez M. and Graham M. D., *Phys. Fluids*, **19** (2007) 073602.

[18] Rusconi R. and Stone H. A., *Phys. Rev. Lett.*, **101** (2008) 254502.

[19] Leshansky A. M., Morris J. F. and Brady J. F., *J. Fluid Mech.*, **597** (2008) 305.

[20] Wedin P. *et al.*, *J. Colloid Interface Sci.*, **272** (2004) 1.

[21] Barenblatt G. I., *Prikl. Mat. Mekh.*, **16** (1952) 67.

[22] Pattle R. E., *Q. J. Mech. Appl. Math.*, **12** (1959) 407.

[23] Bluman G. W. and Kumei S., *J. Math. Phys.*, **21** (1980) 1019.

[24] Belongia B. M. and Baygents J. C., *J. Colloid Interface Sci.*, **195** (1997) 19.

[25] d'Orlyé F., Varenne A. and Gareil P., *J. Chromatogr. A*, **1204** (2008) 226.